

## Intralayer and interlayer exchange tuned by magnetic field in the bilayer manganite $(\text{La}_{0.4}\text{Pr}_{0.6})_{1.2}\text{Sr}_{1.8}\text{Mn}_2\text{O}_7$ probed by inelastic neutron scattering

F. Moussa,<sup>1</sup> M. Hennion,<sup>1</sup> A. Gukasov,<sup>1</sup> S. Petit,<sup>1</sup> L. P. Regnault,<sup>2,3</sup> A. Ivanov,<sup>2</sup> R. Suryanarayanan,<sup>4</sup> M. Apostu,<sup>4</sup> and A. Revcolevschi<sup>4</sup>

<sup>1</sup>Laboratoire Léon Brillouin, CEA-CNRS, CEA-Saclay, F-91191 Gif-sur-Yvette Cedex, France

<sup>2</sup>Institut Laue-Langevin, B.P. 156 X, F-38042 Grenoble Cedex 9, France

<sup>3</sup>CEA-Grenoble, INAC-SPSMS-MDN, 38054 Grenoble Cedex 9, France

<sup>4</sup>Laboratoire de Physico-Chimie de l'Etat Solide, Université Paris-Sud, URM CNRS 8182, F-91405 Orsay Cedex, France

(Received 13 May 2008; revised manuscript received 16 July 2008; published 20 August 2008)

The bilayer manganite  $\text{La}_{1.2}\text{Sr}_{1.8}\text{Mn}_2\text{O}_7$  (LSMO) exhibits a phase transition from a paramagnetic insulating (PI) to a ferromagnetic metallic (FM) state with a colossal magnetoresistance (CMR) effect. Upon 60% Pr substitution, both the magnetic order and the PI to FM transition are suppressed. However, application of a magnetic field induces a first-order transition to a FM state with a CMR effect. We report here inelastic neutron scattering from a single crystal of  $(\text{La}_{0.4}\text{Pr}_{0.6})_{1.2}\text{Sr}_{1.8}\text{Mn}_2\text{O}_7$  under a magnetic field of 3.7 T, applied along the  $c$  axis and along the  $[110]$  direction. Our data reveal the in-plane exchange  $J_{ab}$  close to that of the Pr-free compound LSMO although the interlayer exchange  $J_c$  is much smaller than that found in LSMO. Anisotropic lattice distortion induced by the smaller size of  $\text{Pr}^{3+}$  ion is considered to explain these results.

DOI: 10.1103/PhysRevB.78.060406

PACS number(s): 75.47.Lx

Systems showing a phase transition from a paramagnetic insulating (PI) to a ferromagnetic metallic (FM) state, tuned by magnetic field, have drawn considerable interest both from applications and fundamental points of view. The  $(\text{La}_{0.4}\text{Pr}_{0.6})_{1.2}\text{Sr}_{1.8}\text{Mn}_2\text{O}_7$  (LPSMO) compound, discovered in the early 2000s,<sup>1,2</sup> belongs to this category. It derives from the  $n=2$  member of the Ruddlesden-Popper series expressed generally as  $(\text{La}_{1-x}\text{Sr}_x)_{n+1}\text{Mn}_n\text{O}_{3n+1}$ . The bilayer compound with  $n=2$  and, for the hole doping,  $x=0.4$  shows a PI-FM transition at  $T_C=125$  K with a magnetoresistance ratio of  $\sim 180$ .<sup>3-5</sup> Keeping the hole doping constant at  $x=0.4$  but with an additional substitution of Pr on the La site, viz.  $(\text{La}_{0.4}\text{Pr}_{0.6})_{1.2}\text{Sr}_{1.8}\text{Mn}_2\text{O}_7$ , the material becomes a paramagnetic insulator at all temperatures. However an applied magnetic field induces a first-order PI to FM transition. A previous inelastic neutron-scattering experiment<sup>6</sup> with a magnetic field  $\mathbf{H}$  along the  $c$  axis has revealed that the magnetic field restores not only a long-range ferromagnetic order but also an exchange coupling between in-plane first neighbors,  $J_{ab}$ , very similar to that of  $\text{La}_{1.2}\text{Sr}_{1.8}\text{Mn}_2\text{O}_7$  (LSMO). Both the interlayer and intralayer couplings are expected to play a role in the formation of magnetic and transport properties of this bilayer compound. Hence, further inelastic neutron-scattering experiments on LPSMO have been achieved to evaluate the intralayer exchange coupling  $J_{ab}$  and the interlayer exchange coupling  $J_c$ , or rather  $SJ_{ab}$  and  $SJ_c$  with  $S$  as the mean localized spin of the Mn ion, in a magnetic field of 3.7 T and at 15 K (see Fig. 1).

Our studies reveal that the field-induced coupling is independent of the field direction ( $\mathbf{H}\parallel\mathbf{c}$  and  $\mathbf{H}\parallel\mathbf{a}+\mathbf{b}$ ). Furthermore, we found that the intralayer value  $SJ_{ab}$  of our sample is comparable to that of LSMO (Refs. 7 and 8) whereas the interlayer value  $SJ_c$  is strongly reduced. Another important finding concerns an interesting evolution of the ground state of the  $\text{Pr}^{3+}$  ion with the direction of the field  $H$ . With  $\mathbf{H}\parallel\mathbf{a}+\mathbf{b}$ , we have measured, in addition to the spin waves, an excitation at 8 meV that we have identified with a crystal-

field excitation of  $\text{Pr}^{3+}$ . With  $\mathbf{H}\parallel\mathbf{c}$ , this excitation was not seen.

The high quality single crystal of LPSMO studied in this work was the same as the one described in Ref. 6. The space group of the structure is  $I4/mmm$  with  $a=b\approx 3.85$  Å and  $c\approx 20$  Å. The sample was mounted on an aluminum holder in a horizontal field superconducting magnet. The sample was aligned with its  $(\mathbf{a}+\mathbf{b})$  and  $\mathbf{c}$  scattering plane horizontal and the magnetic field was being applied either parallel to  $c$  or to  $\mathbf{a}+\mathbf{b}$  with  $H=3.7$  T. With  $\mathbf{H}\parallel\mathbf{c}$ , the transition temperature from PI to FM phase  $T_C$  is  $\approx 72$  K while with  $\mathbf{H}\parallel\mathbf{a}+\mathbf{b}$ , at this value,  $T_C\approx 64$  K.

Elastic and inelastic neutron-scattering measurements have been carried out on the triple axis spectrometers IN22 and IN8 of the Institut Laue-Langevin in Grenoble. For the inelastic measurements, the momentum transfer  $\mathbf{Q}$  was kept close to the direction of the magnetic field in order to take advantage of the geometrical rule of the neutron magnetic cross section, which is proportional to the spin components perpendicular to  $\mathbf{Q}$ .<sup>9</sup>

The double exchange (DE) model is appropriate to describe magnetic interactions in colossal magnetoresistance (CMR) manganites.<sup>10</sup> It turns out that the spin-wave disper-

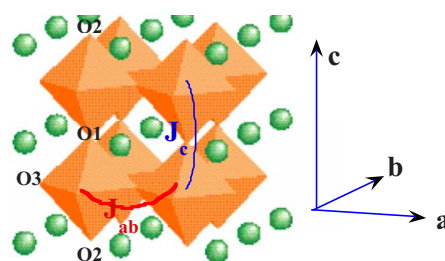


FIG. 1. (Color online) Structure of the bilayer compound. Mn ions (not shown) are at the center of  $\text{MnO}_6$  octahedra, coupled by intralayer  $J_{ab}$  and interlayer  $J_c$ . For a general view of the structure, see Refs. 8, 19, and 21.

sion for this DE model in the  $J_H = \infty$  limit is precisely the same as that for the Heisenberg ferromagnetic model (HFM). Thus, in order to analyze the data, we considered the Hamiltonian of the HFM model with two distinct exchange couplings between nearest neighbors: the intralayer exchange integral  $J_{ab}$ , coupling in-plane Mn sites, and the interlayer exchange integral  $J_c$ , coupling Mn sites belonging to the two layers forming the bilayer. Let us note that the interbilayer coupling is  $\approx 100$  times smaller than  $J_c$ ,<sup>7</sup> which is below the sensitivity of our experiment. For the HFM model, the dispersion of the spin waves propagating in the  $(\mathbf{a}, \mathbf{b})$  plane consists of two branches: an acoustic one,  $\omega(q)_{ac}$ , and an optic one,  $\omega(q)_{opt}$ :

$$\omega_{ac}(\mathbf{q}) = \omega_0 + 4SJ_{ab}[\sin^2(\pi q_x) + \sin^2(\pi q_y)],$$

$$\omega_{opt}(\mathbf{q}) = \omega_{ac}(\mathbf{q}) + 2SJ_c,$$

where  $\omega_0$  is a gap due to intrinsic anisotropy (see Ref. 6).

We define, with  $\boldsymbol{\tau}$  in the  $I4/mmm$  indexation,

$$\mathbf{Q} = \boldsymbol{\tau} + \mathbf{q},$$

$$\mathbf{Q} = \left[ \frac{2\pi}{a}(H + q_x, K + q_y), \frac{2\pi}{c}Q_L \right],$$

$$Q_Z = \frac{2\pi}{c}Q_L.$$

In the selected crystal orientation,  $q_x = q_y$ . The intensities of both spin-wave branches are given by the neutron magnetic inelastic cross section:

$$\begin{aligned} \frac{d^2\sigma}{d\Omega d\omega} &= \frac{k_f}{k_i} (r_0)^2 \frac{S}{2} |F(Q)|^2 \left[ 1 + \left( \frac{Q_{\parallel}}{Q} \right)^2 \right] \\ &\times \left[ \cos^2 \left( \frac{Q_Z \Delta z}{2} \right) \mathcal{S}^{ac}(\mathbf{Q}, \omega) \right. \\ &\left. + \sin^2 \left( \frac{Q_Z \Delta z}{2} \right) \mathcal{S}^{opt}(\mathbf{Q}, \omega) \right], \end{aligned}$$

where

$$\mathcal{S}^{ac, opt}(\mathbf{Q}, \omega) = [n(\omega) + 1] \chi''_{ac, opt}(\mathbf{Q}, \omega)$$

with

$$\begin{aligned} \chi''_{ac, opt}(\mathbf{Q}, \omega) &\propto \frac{\Gamma(q)}{[\omega - \omega_{ac, opt}(q)]^2 + \Gamma(q)^2} \\ &- \frac{\Gamma(q)}{[\omega + \omega_{ac, opt}(q)]^2 + \Gamma(q)^2}, \end{aligned}$$

$k_i$  is the incident neutron wave vector,  $k_f$  the scattered-neutron wave vector,  $r_0 = 0.5410^{-12}$  cm,  $n(\omega)$  the Bose factor,  $S$  the spin,  $F(Q)$  the magnetic form factor of the Mn ion,  $Q_{\parallel}$  is the  $Q$  component parallel to the magnetic field  $H$ , and  $\Delta z$  the thickness of the bilayer with  $\Delta z \approx a$ . The possibility of finite spin-wave lifetimes  $1/\Gamma(q)$  was allowed for replacing the delta-function response with Lorentzian functions<sup>11</sup> in the neutron cross section. The intensity of the acoustic branch is maximum for

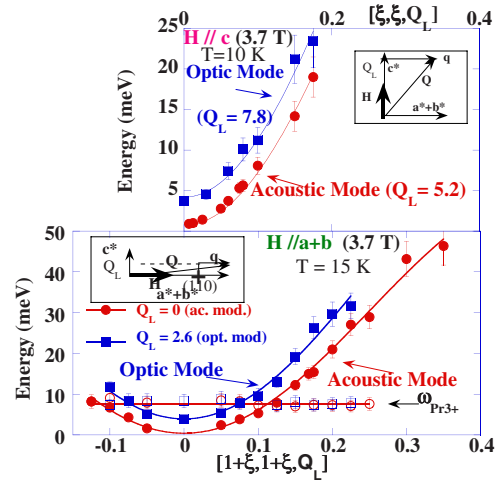


FIG. 2. (Color online) Dispersion of spin waves propagating along  $[110]$ . Acoustic branch: solid dots. Optic branch: solid squares. The solid lines represent the laws  $\omega_{ac}(q)$  and  $\omega_{opt}(q)$ . Upper panel:  $\mathbf{H} \parallel \mathbf{c}$ ; lower panel:  $\mathbf{H} \parallel \mathbf{a} + \mathbf{b}$ . Crystal field excitation  $\omega_{Pr3+}$ : empty symbols.

$$\frac{Q_Z \Delta z}{2} = 0, \pi, 2\pi, \dots,$$

$$Q_L = 0, \frac{c}{a}, \frac{2c}{a}, \dots = 0, 5.2, 10.4, \dots,$$

and that of the optic one for

$$\frac{Q_Z \Delta z}{2} = \frac{\pi}{2}, \frac{3\pi}{2}, \dots,$$

$$Q_L = \frac{c}{2a}, \frac{3c}{2a}, \dots = 2.6, 7.8, \dots$$

The inelastic spectra were described with this cross section, convoluted with the instrumental resolution function. In all the spectra represented, the lines through the points were the results of a fitting process with  $\omega_{ac, opt}(q)$  and  $\Gamma(q)$ , the damping constant of spin waves, as fitting parameters. Concerning this last point, at the temperature of the study (15 K), the spin waves were always underdamped ( $\Gamma(q) < \omega_{ac, opt}$ ).

Figure 2 displays the dispersion of spin waves propagating in the basal plane  $(\mathbf{ab})$  for  $\mathbf{H} \parallel \mathbf{c}$  (upper panel) and  $\mathbf{H} \parallel \mathbf{a} + \mathbf{b}$  (lower panel). Taking advantage of the modulation of the intensity with  $Q_L$  as in the case of  $\mathbf{H} \parallel \mathbf{c}$ , energy scans were performed at constant  $\mathbf{Q} = (\xi, \xi, Q_L)$  with  $Q_L = 5.2$  to measure acoustic modes and  $Q_L = 7.8$  for optic modes (Fig. 2, upper panel). In the case of  $\mathbf{H} \parallel \mathbf{a} + \mathbf{b}$ , the scans were measured at  $\mathbf{Q} = (1 + \xi, 1 + \xi, Q_L)$  with  $Q_L = 0$  for acoustic modes and  $Q_L = 2.6$  for optic modes (Fig. 2, lower panel). A typical spectrum of the optic mode at  $\mathbf{Q} = (0, 0, 7.8)$  with  $\mathbf{H} \parallel \mathbf{c}$  is shown in the left panel (solid symbols) of Fig. 3. To prove that this mode is related to the interaction of the first neighbor Mn ions in the two adjacent layers forming the bilayer, we performed a constant-energy scan along  $[001]$  (shown in Fig. 3, right panel).

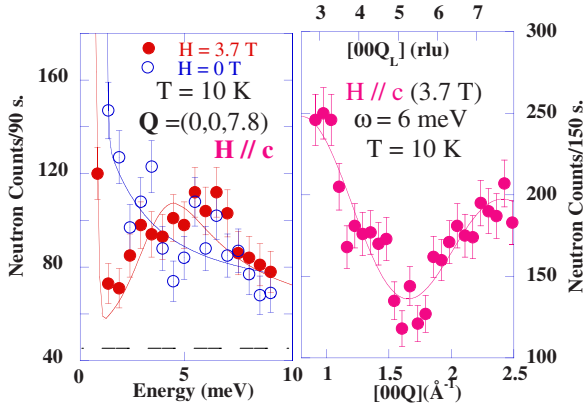


FIG. 3. (Color online) Left panel: Spectra of the optic mode at  $q_x=q_y=0$  with  $\mathbf{H}\parallel\mathbf{c}$  (solid dots) and without magnetic field (empty dots). Broken line represents the instrument background. Right panel: Intensity of the optic mode versus  $Q_L$  at constant energy  $\omega=6$  meV. This value has been chosen because it corresponded to the maximum measured intensity (see left panel). Solid lines represent the best fits, as explained in the text.

The solid line through the experimental points is calculated using the given formula for the neutron cross section. The fitted periodicity is  $Q_L=5.2$  or  $Q_Z=5.2\times 2\pi/c=1.63\text{ \AA}^{-1}$ . It corresponds to a wavelength  $\lambda=2\pi/Q_Z\approx 3.85\text{ \AA}$ , which is exactly  $\Delta z$ : the thickness of the bilayer.

With  $\mathbf{H}\parallel\mathbf{a}+\mathbf{b}$ , as can be seen in the lower panel of Fig. 2, the spin-wave branches appear very similar to the case where  $\mathbf{H}\parallel\mathbf{c}$ , except, however, for an additional flat mode  $\omega_{\text{Pr}^{3+}}$  at  $\approx 8$  meV. We have identified this latter mode with a crystal-field excitation of the  $\text{Pr}^{3+}$  ion for several reasons: (i) the absence of dispersion of this mode. (ii) From a previous polarized neutron experiment,<sup>12</sup> we know that, when  $\mathbf{H}\parallel\mathbf{a}+\mathbf{b}$ , all  $\text{Pr}^{3+}$  ions are in a singlet (nonmagnetic) state so transition to an excited magnetic state is possible, as already observed in other Pr compounds.<sup>13,14</sup> A typical energy scan is shown in the left panel of Fig. 4.

One can see clearly a spin-wave acoustic mode  $\omega_{ac}$  and a much less intense mode  $\omega_{\text{Pr}^{3+}}$  (solid symbols). In the small energy range, whereas this flat mode is well distinct from the acoustic branch, this is not the case for the optic branch, which has a lower intensity. However, from the whole set of data, we could extract the optic branch. Due to the proximity of this flat mode, the constant-energy scan (such as that displayed in Fig. 3, right panel) could not be performed. We present the evolution of the intensity (with  $Q_L$ ) of an acoustic mode at a constant energy of 4 meV (Fig. 4, right panel). The intensity is maximum at  $q_x=q_y=0.075$  and  $Q_L=0$ , and shows the periodicity already found ( $Q_L=5.2$ ) but, in that case, in phase opposition with the scan of the optic mode reported in the right panel of Fig. 3, as expected.

When the magnetic field is switched off, the system becomes paramagnetic. The spin-wave mode transforms into a diffusive mode, giving rise to quasielastic scattering (Figs. 3 and 4, empty symbols), while  $\omega_{\text{Pr}^{3+}}$  still remains (Fig. 4).<sup>15</sup>

Using the expressions of  $\omega_{ac}(\mathbf{q})$  and  $\omega_{\text{opt}}(\mathbf{q})$ , we could extract the values of  $SJ_{ab}$  and  $SJ_c$  from our experimental data. For each orientation of the field,  $SJ_{ab}$  has been determined from the dispersion of both branches.  $SJ_c$  has been

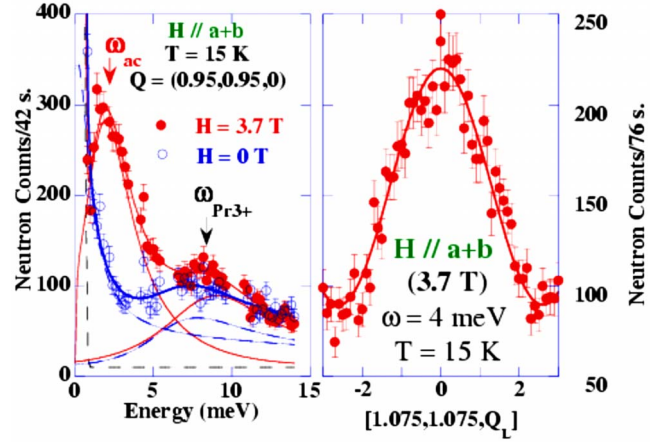


FIG. 4. (Color online) Left panel: Energy spectrum measured at  $Q=(0.95,0.95,0)$  with  $\mathbf{H}\parallel\mathbf{a}+\mathbf{b}$  (solid dots) and without magnetic field (empty dots). In the latter case,  $\omega_{ac}$  disappears while  $\omega_{\text{Pr}^{3+}}$  remains visible. Right panel: Intensity of an acoustic mode versus  $Q_L$  at  $Q_x=Q_y=1.075$  and at constant energy  $\omega=4$  meV. The solid line represents the best fit (see the text).

determined by the mode at  $q=0$  on the optic branch:  $\omega_{\text{opt}}(\mathbf{q}=0)=\omega_0+g\mu_B H+2SJ_c$ , where  $\omega_0$  is due to a single-ion anisotropy and  $g\mu_B H$  the Zeeman energy (with  $H=3.7$  T  $g\mu_B H=0.428$  meV). The precision of the determination of  $J_c$  depends on the knowledge of  $\omega_0$ . In the case of  $\mathbf{H}\parallel\mathbf{c}$ ,  $\omega_0$  was pretty well known because of its precise measurement on a cold neutron triple axis spectrometer,  $\omega_0=0.29$  meV.<sup>6</sup> This was not the case for  $\mathbf{H}\parallel\mathbf{a}+\mathbf{b}$  since the measurements were performed on thermal-neutron triple axis spectrometers. However, the fit of our data (Fig. 2, solid red circles) has yielded  $\omega_0=0.14\pm 0.14$  meV. This is in good agreement with what is known in this compound, namely that the magnetic anisotropy is strongest with  $H$  along  $\mathbf{c}$  (see Ref. 1 and more recently, Ref. 16). The values of  $SJ_{ab}$  and  $SJ_c$  are presented in the Table I, and compared with the values found in the literature for the Pr-free compound LSMO.

The first observation is that the set of values of exchange couplings for LPSMO does not vary very much with the direction of the magnetic field. It is hard to say that  $J_{ab}$  is smaller in the case of  $\mathbf{H}\parallel\mathbf{a}+\mathbf{b}$ , as it is at the limit of the error bars.

The second observation concerns the comparison of these results with those of the parent Pr-free compound LSMO. The intralayer exchange coupling  $SJ_{ab}$  is nearly the same in both compounds while the interlayer exchange coupling  $SJ_c$  is very different. Moreover, the ratios of  $T_C$  (125/72) and of  $J_c$  (3/1.7) are the same, and equal to 1.7. This last result can

TABLE I. See text.

	$SJ_{ab}(\text{meV})$	$SJ_c(\text{meV})$	$T_C(\text{K})$
LPSMO $\mathbf{H}\parallel\mathbf{c}$	$8.9\pm 0.35$	$1.7\pm 0.2$	72
LPSMO $\mathbf{H}\parallel\mathbf{a}+\mathbf{b}$	$8.2\pm 0.3$	$1.7\pm 0.3$	64
LSMO	8.64 (Ref. 7), 9.6 (Ref. 8)	3.06 (Ref. 7), 2.9 (Ref. 8)	125 (Refs. 7 and 8)

be well explained by a calculation of  $T_C$  based on a Wilson-Kadanoff argument, developed for a quasibidimensional Heisenberg model<sup>17</sup> where  $T_C$  is shown to vary as  $J_c$ . However, why is the intralayer exchange coupling  $J_{ab}$  very close in both compounds and why is the interlayer coupling  $J_c$  so different? The small size of the Pr ion is usually invoked to explain why Pr substitution on the La site in the parent bilayer compound destroys ferromagnetic order. The ionic radius of  $\text{Pr}^{3+}$  is nearly 6% smaller than that of  $\text{La}^{3+}$  (Ref. 18) so the structure is distorted, the electronic band is narrower, and the system becomes paramagnetic and insulating. However, the energies of different possible ground states are very close to each other and the delicate balance existing between these states can be easily tipped by a magnetic field. Considering the FM phase of the Pr-free compound, one observes that it is also distorted with elongated  $\text{MnO}_6$  octahedra along **c** (Ref. 19) and that the interlayer exchange coupling  $J_c$ , unlike  $J_{ab}$ , is very sensitive to the doping rate.<sup>8</sup> In the present case of LPSMO, Pr substitution dramatically changes the physical properties.<sup>20,21</sup> For both compounds, the (**ab**) planes consist of long-range ordered squares with an edge  $\text{Mn-O3-Mn} \approx 3.85 \text{ \AA}$  (see Fig. 1). This square structure is very robust against any perturbation; the electron density remains stable and, as a consequence,  $J_{ab}$  remains constant. On the contrary, the stacking of bilayers along the *c* axis is much

less dense; the first neighbor bilayers are distant of  $\approx 10 \text{ \AA}$ , making the bilayer more isolated, more fragile, and easily buckled. The randomly distributed Pr ions induce fluctuations in the positions of oxygen atoms outside the bilayer, O2, leading to elongated octahedra along the **c** axis. As such, the thickness of the bilayer “O2-Mn-O1-Mn-O2” fluctuates. This, in turn, likely leads to fluctuations in the electronic density that, in addition to the disorder, can reduce the ferromagnetic coupling along the *c* direction. As such, the distortions induced by the Pr ions, although reduced by the applied magnetic field, remain strong enough along the *c* axis to prevent a complete restoration of the magnetic coupling  $J_c$ , resulting in a reduction in  $T_C$  in comparison with LSMO (see Table I).

In summary, we have measured the highly anisotropic exchange coupling constants  $J_{ab}$  (intralayer coupling) and  $J_c$  (interlayer coupling) in the field-induced ferromagnetic metallic phase of the bilayered Pr-substituted compound  $(\text{La}_{0.4}\text{Pr}_{0.6})_{1.2}\text{Sr}_{1.8}\text{Mn}_2\text{O}_7$ . We found that the values of  $J_{ab}$  and  $J_c$  are not sensitive to the direction of the applied field whether *H* is along **c** or along **a+b**. Whereas the value determined for  $J_{ab}$  is very close to that of the Pr-free compound LSMO, the value for  $J_c$  is remarkably smaller. We attribute our findings to the strong anisotropic distortions induced by the Pr ions.

- 
- <sup>1</sup>M. Apostu, R. Suryanarayanan, A. Revcolevschi, H. Ogasawara, M. Matsukawa, M. Yoshizawa, and N. Kobayashi, *Phys. Rev. B* **64**, 012407 (2001).
- <sup>2</sup>I. Gordon, P. Wagner, V. V. Moshchalkov, Y. Bruynseraede, M. Apostu, R. Suryanarayanan, and A. Revcolevschi, *Phys. Rev. B* **64**, 092408 (2001).
- <sup>3</sup>Y. Moritomo, A. Asamitsu, and H. Kuwahara, *Nature (London)* **380**, 141 (1996).
- <sup>4</sup>T. Kimura, Y. Tomioka, H. Kuwahara, A. Asamitsu, M. Tamura, and Y. Tokura, *Science* **274**, 1698 (1996).
- <sup>5</sup>T. Kimura, Y. Tomioka, A. Asamitsu, and Y. Tokura, *Phys. Rev. Lett.* **81**, 5920 (1998).
- <sup>6</sup>F. Moussa, M. Hennion, F. Wang, A. Gukasov, R. Suryanarayanan, M. Apostu, and A. Revcolevschi, *Phys. Rev. Lett.* **93**, 107202 (2004).
- <sup>7</sup>T. Chatterji, L. P. Regnault, P. Thalmeier, R. Suryanarayanan, G. Dhahenne, and A. Revcolevschi, *Phys. Rev. B* **60**, R6965 (1999); T. Chatterji, P. Thalmeier, G. J. McIntyre, R. van de Kamp, R. Suryanarayanan, G. Dhahenne, and A. Revcolevschi, *Europhys. Lett.* **46**, 801 (1999).
- <sup>8</sup>T. G. Perring, D. T. Adroja, G. Chaboussant, G. Aeppli, T. Kimura, and Y. Tokura, *Phys. Rev. Lett.* **87**, 217201 (2001).
- <sup>9</sup>S. W. Lovesey, *Theory of Neutron Scattering From Condensed Matter* (Clarendon, Oxford, 1987).
- <sup>10</sup>N. Furukawa, *J. Phys. Soc. Jpn.* **65**, 1174 (1996).
- <sup>11</sup>I. A. Zaliznyak, L.-P. Regnault, and D. Petitgrand, *Phys. Rev. B* **50**, 15824 (1994).
- <sup>12</sup>F. Wang, A. Gukasov, F. Moussa, M. Hennion, M. Apostu, R. Suryanarayanan, and A. Revcolevschi, *Phys. Rev. Lett.* **91**, 047204 (2003).
- <sup>13</sup>K. C. Turberfield, L. Passell, R. J. Birgeneau, and E. Bucher, *J. Appl. Phys.* **42**, 1746 (1971).
- <sup>14</sup>A. T. Boothroyd, S. M. Doyle, D. M. Paul, and R. Osborn, *Phys. Rev. B* **45**, 10075 (1992).
- <sup>15</sup>When the field was removed, before measuring at low temperature, the single crystal was heated at a temperature of  $\approx 90\text{K} \gg T_C$ .
- <sup>16</sup>M. Matsukawa, Y. Yamato, T. Kumagai, A. Tamura, R. Suryanarayanan, S. Nimori, M. Apostu, A. Revcolevschi, K. Koyama, and N. Kobayashi, *Phys. Rev. Lett.* **98**, 267204 (2007).
- <sup>17</sup>F. Moussa and J. Villain, *J. Phys. C* **9**, 4433 (1976).
- <sup>18</sup>D. Kumar, R. K. Singh, and C. B. Lee, *Phys. Rev. B* **56**, 13666 (1997).
- <sup>19</sup>J. F. Mitchell, D. N. Argyriou, J. D. Jorgensen, D. G. Hinks, C. D. Potter, and S. D. Bader, *Phys. Rev. B* **55**, 63 (1997).
- <sup>20</sup>M. Matsukawa, A. Tamura, S. Nimori, R. Suryanarayanan, T. Kumagai, Y. Nakanishi, M. Apostu, A. Revcolevschi, K. Koyama, and N. Kobayashi, *Phys. Rev. B* **75**, 014427 (2007).
- <sup>21</sup>A. Gukasov, F. Wang, B. Anghoefler, L. He, R. Suryanarayanan, and A. Revcolevschi, *Phys. Rev. B* **72**, 092402 (2005).